

Cite this: *Nanoscale Adv.*, 2021, 3, 3298

# An ambient complexation reaction of zinc acetate and ascorbic acid leads to a new form of nanoscale particles with emergent optical properties†

Srestha Basu,‡<sup>a</sup> Archismita Hajra <sup>‡b</sup> and Arun Chattopadhyay <sup>\*ab</sup>

We report the formation of nanoscale particles from the complexation reaction between zinc acetate and ascorbic acid under ambient conditions and in an aqueous medium. The reaction led to the formation of a molecular complex with the formula  $Zn_x(AA)_y(OAc)_z$  ( $x$ ,  $y$ , and  $z$  = possible smallest positive integer) with AA meaning ascorbate, based on the mass spectrometry results. Following this, the formation of luminescent nanoscale particles – the size of which increased with time – was observed. During 24 h of observation, the sizes increased to about 50 nm in the presence of different sizes at all times. Transmission electron microscopy results also indicated the formation of polycrystalline as well as amorphous nanoparticles in the medium. Further, the appearance of a UV absorption peak at 380 nm and photoluminescence peak at 473 nm marked the formation of the nanoparticles. The luminescence was also observed to be wavelength tuneable. FTIR and NMR spectroscopy results also supported the formation of a molecular complex with the above formula. The present work highlights the importance of emergent properties of nanoscale molecular materials for crystallization. Also, the present discovery is expected to contribute to the development of safe nanomaterials.

Received 9th January 2021  
Accepted 6th April 2021DOI: 10.1039/d1na00023c  
[rsc.li/nanoscale-advances](http://rsc.li/nanoscale-advances)

## Introduction

Advancements in nanoscale science and technology have continuously been supplemented by the discovery of new species with extraordinary properties.<sup>1–6</sup> Amongst them, colloidal gold (Au) has been known since antiquity; however, its optical properties have been explained based on light scattering about a hundred years back. On the other hand, its dimension-dependent properties at the nanoscale have been realized recently through the syntheses of well-defined structures.<sup>7</sup> The knowledge has helped reveal the potential of nanoscale Au particles in fields as diverse as catalysis,<sup>8</sup> healthcare<sup>9,10</sup> and optoelectronics.<sup>11</sup> In that respect, colloidal semiconductor quantum dots (Qdots) and their counterparts fabricated using top-down approaches have generated much excitement in a wide range of fields as mentioned above, leading to the commercialization of display devices.<sup>12,13</sup> Additionally, iron oxide nanoparticles are well-known for their superparamagnetic properties at the nanoscale dimensions.<sup>14,15</sup> Similarly, allotropes of carbon such as  $C_{60}$ ,<sup>16</sup> carbon nanotubes<sup>17</sup> and

graphene<sup>18</sup> have received great attention as new materials of choice due to their potential applications. The realization of two-dimensional (2D) graphene has helped expand the repertoire in terms of new materials such as silicene, germanene and 2D  $MoS_2$ .<sup>19,20</sup>

On the other hand, the synthetic chemistry repertoire has been helpful in expanding the reach of nanoscale materials. For example, perovskite nanostructures, carbon nanodots and nanoscale metal organic and similar frameworks have given rise to a plethora of potentials especially applicable in the fields of healthcare, energy and the environment.<sup>21–23</sup> Further, DNA-based nanostructures are shown to have important application potentials in healthcare, especially targeted delivery and probes.<sup>24–26</sup> Inorganic nanoparticles are known to typically display dimension dependent physical and chemical properties. Organic nanoparticles such as liposomes, dendrimers, micelles and proteins do not display such properties.<sup>27</sup> On the other hand, they can be excellent choices for size dependent drug delivery, host for water insoluble drugs and in addition, they can be used as templates for size and shape selected synthesis of inorganic nanoparticles.<sup>28–30</sup> Notably, the field of molecular nanoparticles has also witnessed extensive growth in the recent past. For instance, crystalline luminescent nanoparticles of organic molecules have been developed following confinement of amorphous nanoparticulate molecules in a rigid polymer matrix and subsequential treatment with solvent vapor. The organic molecules were found to exhibit augmented luminescence in the nanoparticulate form.

<sup>a</sup>Department of Chemistry, Indian Institute of Technology Guwahati, Guwahati 781039, India

<sup>b</sup>Centre for Nanotechnology, Indian Institute of Technology Guwahati, Guwahati 781039, India

† Electronic supplementary information (ESI) available. See DOI: 10.1039/d1na00023c

‡ Equal contribution.



Moreover, colloidal nanoscale particles of zwitterionic molecules have been synthesised *via* the reprecipitation method assisted by polyelectrolytes.<sup>31,32</sup> In addition, molecules exhibiting aggregation induced emission can be tailored to synthesize such nanoscale particles for imaging probes and other optoelectronic applications.<sup>33,34</sup>

The proposition that molecular nanotechnology could revolutionize the bottom-up approaches in the manufacturing of advanced materials and devices needs novel strategies not only in bond making and breaking but also in interactions between chemical bonds that will help design objects at the highest resolution. In this regard, the development of important structures such as rotaxane and catenane has given rise to the excitement of building machines and their components with precision at the scale of a molecular bond.<sup>35,36</sup> However, whether such a principle could lead to viable devices is still an open question, given the complexity of chemical interactions at the molecular level. Thus, the growth of the repertoire of molecules, methods and their assemblies in diverse dimensions ought to continue with the arrival of new methods, molecules and materials. In this regard, the development of nanoscale particles based on interactions amongst inorganic complexes could bring new properties, which may be useful in molecular nanotechnology. For examples, the as-synthesized inorganic metal complexes may interact in a liquid medium and give rise to the formation of nanoscale particles with emergent properties that are not present in the complexes themselves. This may pave a new way of assembly based on interacting complexes with each component contributing chemical and physical properties based on the metal center and its oxidation state and the ligand of choice. The emergent properties may or may not have the signatures of the participating complexes. However, given the molecular nature of the interactions, an appropriate choice could be made leading to specific interactions in three dimensions. Such an approach is yet to be reported in the literature.

Herein we report the unprecedented emergence of photoluminescence of nanoscale assembly of metal complexes when the reaction was carried out in an aqueous medium. Thus, chemical reactions – under ambient conditions – involving ascorbic acid and zinc acetate in the aqueous medium led to the formation of the  $Zn_x(AA)_y(OAc)_z$  complex; AA is ascorbate. The so-formed complex resulted in the formation of nanoscale particles with time, having strong luminescence in the blue region of wavelengths. The formation of the complex was ascertained by mass spectrometry and NMR spectroscopy analyses. The formation of nanoscale particles was confirmed by transmission electron microscopy. Such analysis also revealed both the polycrystalline and amorphous nature of the particles formed in the dispersion medium. Interestingly, the luminescence was observed to be dependent on the excitation wavelength similar to the observations in carbon dots. Time resolved photoluminescence measurements indicated gradual shortening of the lifetime of the excited state, thus indicating interactions amongst the complexes leading to the formation of nanoparticles. Further, FTIR analysis indicated possible coordination of hydroxyl groups of ascorbate and acetate with zinc ions, leading to the formation of the complex mentioned above.

Also, the role of hydrogen bonding for the association of  $Zn_x(-AA)_y(OAc)_z$  moieties, resulting in the formation of nanoparticles, was evident from the FTIR analysis.

## Results and discussion

Addition of zinc acetate to an aqueous solution of ascorbic acid led to the formation of a colorless dispersion. Initially, the absorbance spectrum of the dispersion did not consist of any discernible peak in the range of spectral acquisition (325 nm to 450 nm). However, with time, the UV-vis absorbance of the reaction mixture increased with the emergence of a peak centred at 380 nm (Fig. 1A). This indicated the possible formation of an additional chemical species (reaction product or intermediate) in the medium. In order to establish that zinc acetate and ascorbic acid underwent a chemical reaction, time-dependent UV-vis absorbance spectra of ascorbic acid as well as zinc acetate were acquired separately as control experiments (Fig. S1A and B†). Interestingly, no significant peak appeared with time in the absorbance of zinc acetate. In an allied vein, no

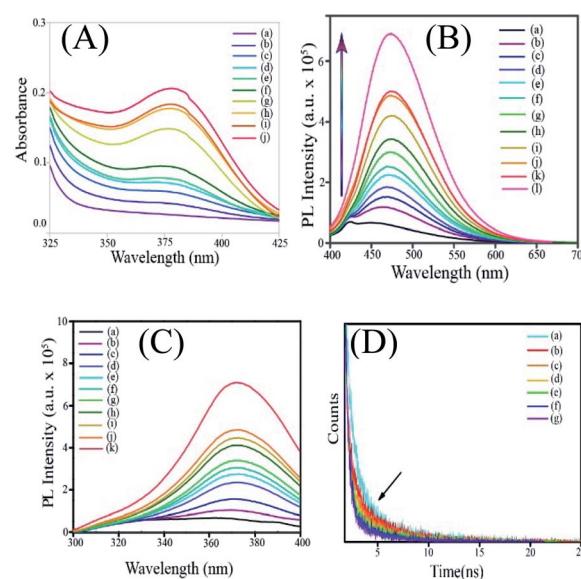


Fig. 1 (A) UV-vis absorbance spectra of the reaction mixture comprising ascorbic acid and zinc acetate dihydrate acquired at (a) 0 min, (b) 20 min, (c) 30 min, (d) 40 min, (e) 50 min, (f) 60 min, (g) 130 min, (h) 3 h, (i) 4 h and (j) 5 h following mixing of ascorbic acid and zinc acetate dihydrate. (B) Luminescence spectra of the reaction mixture comprising ascorbic acid and zinc acetate dihydrate acquired at (a) 0 min, (b) 20 min, (c) 30 min, (d) 40 min, (e) 50 min, (f) 60 min, (g) 130 min, (h) 3 h, (i) 4 h, (j) 5 h, (k) 6 h and (l) 18 h following mixing of ascorbic acid and zinc acetate dihydrate. (C) Luminescence excitation spectra of the reaction mixture comprising ascorbic acid and zinc acetate dihydrate acquired at (a) 0 min, (b) 20 min, (c) 30 min, (d) 40 min, (e) 50 min, (f) 60 min, (g) 130 min, (h) 3 h, (i) 4 h, (j) 5 h and (k) 6 h following mixing of ascorbic acid and zinc acetate dihydrate. The excitation spectra were recorded following fixing of emission at the corresponding emission maximum. (D) Time resolved photoluminescence spectra of the reaction mixture comprising ascorbic acid and zinc acetate dihydrate acquired at (a) 0 min, (b) 17 min, (c) 27 min, (d) 37 min, (e) 47 min, (f) 57 min and (g) 67 min following mixing of ascorbic acid and zinc acetate dihydrate.



significant variation in the absorption characteristics of ascorbic acid was observed in the absence of zinc acetate. The results indicated that zinc acetate and ascorbic acid reacted in the medium and a new species with absorbance in the UV-vis region was formed as a result.

In the next step, the photoluminescence emission and excitation spectra of the dispersion containing ascorbic acid and zinc acetate dihydrate were recorded. Interestingly, it was observed that the emergence of the absorbance peak of the reaction mixture at 380 nm was accompanied by photoluminescence (Fig. 1B). Further, the reaction mixture at the initial period following mixing (0–10 min) was weakly emissive with an emission peak at 449 nm. However, with the progress of time, the luminescence of the mixture increased significantly with a simultaneous bathochromic shift of the emission maximum from 449 nm to 471 nm (Fig. S2†). In an allied vein, the excitation spectra of the reaction mixture recorded at regular intervals of time also showed the growth of a peak centered at 371 nm, with the emission wavelength being set at the corresponding maximum (Fig. 1C). It was further observed that the shift in the emission maximum was observed till ~45 min after mixing the precursors, and the intensity continued to increase till ~36 h. It is important to mention here that the optimum concentration of zinc acetate required for the best possible optical properties of the product was decided following several trials. For example, a fixed concentration of ascorbic acid (~18 mg in 10 mL water) was reacted with 20 mg, 100 mg or 200 mg of zinc acetate. The time dependent luminescence spectra corresponding to each concentration of zinc acetate were then acquired (Fig. S3†). As is evident from Fig. S3,† the maximum luminescence at ~36 h (depending on the rate of the reaction) was observed when ~200 mg of zinc acetate – in comparison to the dispersion containing other concentrations – was reacted with ~18 mg of ascorbic acid in 10 mL water. Further, we have monitored the reaction between ~300 mg of zinc acetate dihydrate and ascorbic acid (as above). Importantly, the trend of enhancement in the luminescence of ascorbic acid with a concomitant bathochromic shift, akin to the case of 200 mg of zinc acetate dihydrate, was observed here as well.

The initial low intensity emission peak of the reaction mixture may be attributed to the luminescence of ascorbic acid owing to the presence of  $\pi$  conjugated moieties and heteroatoms. The emission could also originate from the product(s) of the reaction between ascorbic acid and zinc acetate in the medium. In order to verify the role and the presence of both zinc ions and ascorbic acid in the so formed luminescent product(s), control experiments were performed where the same amount of ascorbic acid and zinc acetate were kept separately and their luminescence behaviours were studied. Importantly, no discernible change in the luminescence of either ascorbic acid or zinc acetate was observed with time (Fig. S4A and B†). In order to probe the involvement of zinc ions in the formation of the product(s), time-dependent photoluminescence spectra of each of the mixtures of cobalt acetate and ascorbic acid, nickel acetate and ascorbic acid, and copper acetate with ascorbic acid were recorded (Fig. S5†).

Interestingly, in the absence of zinc ions, weak luminescence with no clear peak as above could be observed. Thus, the observed luminescence could stem from the product(s) of the reaction involving zinc, ascorbate and acetate ions. Importantly, the role of acetate ions as a component of the luminescent species was further supported by the results of the control experiments. For instance, the time-dependent luminescence spectra of mixtures of zinc perchlorate with ascorbic acid and zinc chloride with ascorbic acid (Fig. S6†) indicated no significant alteration in the luminescence of ascorbic acid (Fig. S6†). In order to further highlight the crucial role of acetate ions in the formation of  $Zn_x(AA)_y(OAc)_z$  NPs, an allied reaction was pursued between zinc formate and ascorbic acid. Interestingly, in line with  $Zn_x(AA)_y(OAc)_z$  nanoparticles, the product of the reaction between zinc formate and ascorbic acid featured emerging luminescence with an emission maximum at 471 nm upon excitation at 371 nm (Fig. S7†). Further, to a mixture of zinc chloride and ascorbic acid, which apparently had weak luminescence, sodium acetate was added. Intriguingly, upon addition of sodium acetate, the mixture exhibited a significant enhancement in luminescence (as were evident from the emission and excitation spectra) with a concomitant bathochromic shift in the emission spectrum, akin to that of the dispersion of zinc acetate and ascorbic acid (Fig. S8†). Thus, the notable enhancement in the emission intensity of the reaction system comprising zinc acetate and ascorbic acid with the associated red shift indicated the possible formation of species involving zinc, acetate and ascorbate ions. Furthermore, the time-dependent enhancement of photoluminescence and the

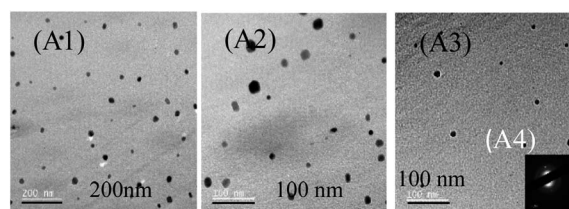


Fig. 2 (A1–A3) Transmission electron microscopy images of the product of the reaction between zinc acetate dihydrate and ascorbic acid acquired over various regions of the TEM grid. (A4) The selected area electron diffraction pattern acquired on a typical particle shown in (A1–A3).

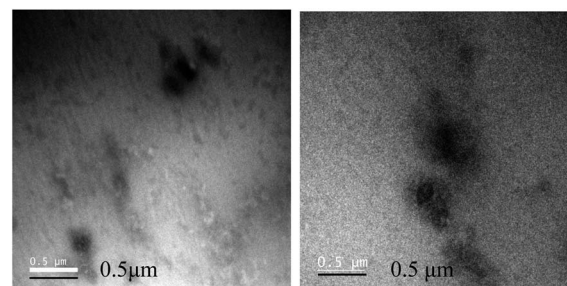


Fig. 3 Transmission electron microscopy images of the reaction mixture comprising zinc acetate dihydrate and ascorbic acid drop cast on the TEM grid at 0 h.



simultaneous gradual bathochromic shift indicated the possible formation of species, whose properties depend on its (their) dimensions. In other words, in the medium, the dimensions of the newly formed species might have changed with time, giving rise to evolving photoluminescence. Further, time-resolved photoluminescence (TRPL) analysis was performed on the samples in a manner similar to that of steady state luminescence and UV-vis absorbance studies (Fig. 1D). Notably, the luminescence lifetime of the system was observed to undergo a sequential decrease with time. For example, the lifetime varied from 2.24 ns to 1.48 ns for samples representing 0 min and 67 min, respectively. This could be attributed to the formation of luminescent species with lower luminescence lifetimes *vis-à-vis* ascorbic acid, as a consequence of the reaction involving zinc, ascorbate and acetate ions. The results also indicated possible size/dimension dependence of the luminescence lifetime of the species so formed in the medium.

Further, TEM analysis was performed to affirm the formation of the nanoparticulate zinc complex. As evinced by TEM analysis, the augmented luminescence of the reaction mixture comprising Zn acetate and ascorbic acid was attributed to the formation of crystalline spherical nanoparticles (Fig. 2A1–A3). Further, the time-dependent red shift observed in the luminescence of the reaction mixture provided an indication of the gradual evolution of the particle size. In order to confirm that, TEM analysis of the reaction mixture collected at regular intervals of time was performed. The results (Fig. 3–7) indicated that the initial reaction mixture (0 h) showed the presence of

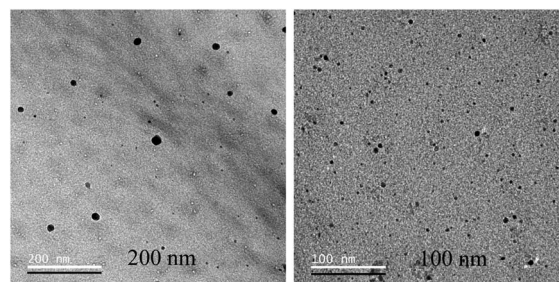


Fig. 6 Transmission electron microscopy images of the reaction mixture comprising zinc acetate dihydrate and ascorbic acid drop cast on the TEM grid at 24 h following mixing of zinc acetate dihydrate and ascorbic acid.

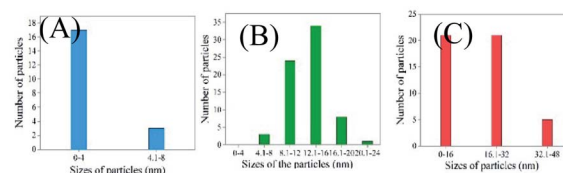


Fig. 7 Size distribution of nanoparticles collected at (A) 40 min, (B) 6 h and (C) 24 h of reaction between zinc acetate dihydrate and ascorbic acid.

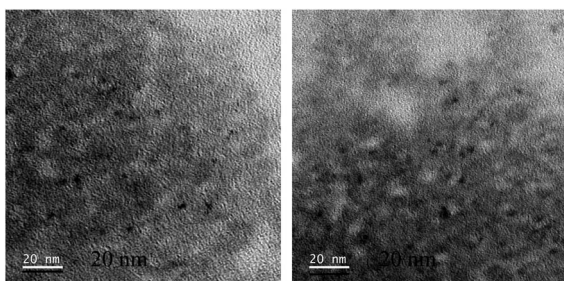


Fig. 4 Transmission electron microscopy images of the reaction mixture comprising zinc acetate dihydrate and ascorbic acid drop cast on the TEM grid at 40 min.

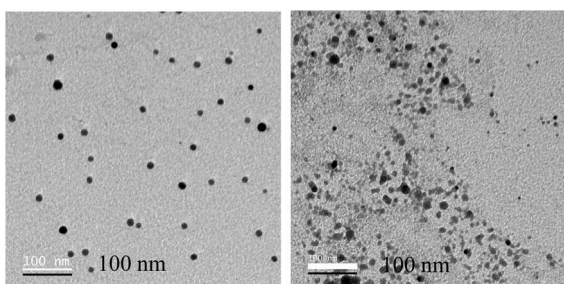


Fig. 5 Transmission electron microscopy images of the reaction mixture comprising zinc acetate dihydrate and ascorbic acid drop cast on the TEM grid at 6 h.

featureless particle like images with no clear contrast (Fig. 3). In other words, at the beginning, the formation of nanoscale particles was not clearly observed. However, that had changed with time (Fig. 4 and 5). For instance, after 40 min of reaction, smaller particles with sizes up to 4 nm could be observed (Fig. 7A). With further progress of the reaction – say at 6 h – larger particles (majority) in the size range of 12 to 16 nm (Fig. 7B) were observed. Finally, after 24 h of reaction, TEM images of the so formed product revealed the presence of even larger particles with sizes up to 48 nm (Fig. 7C). Thus, the gradual enhancement of luminescence of the product of the reaction between ascorbic acid and zinc acetate could be attributed to the formation of nanoscale particles with increasing size, as a function of time of reaction. Also, since the concomitant presence of zinc ions, acetate ions and ascorbate ions were indispensable for the observation of the emergent nanoscale optical properties, the composition of the so formed nanoparticles was likely to involve all the aforementioned chemical species. As evinced by TEM and SAED analyses, the newly formed products showed signatures of both crystalline and amorphous phases. This is clear from the selected area electron diffraction images as reported in the inset of Fig. 2A3 and Table S3.† The X-ray diffraction pattern of the reaction product consisted of the peaks of the precursors greatly, thus discounting the possibility of a real product analysis.

Next, we were interested in identifying the chemical composition of the luminescent nanoparticulate species. In this regard, first, mass spectrometry analysis of the luminescent dispersion was pursued. As is evident from Fig. 8A and B, a peak at 510.8177, corresponding to the presence of  $\text{Zn}_3(\text{AA})(\text{OAc})_2$ , was observed. The experimental mass spectra (isotopic



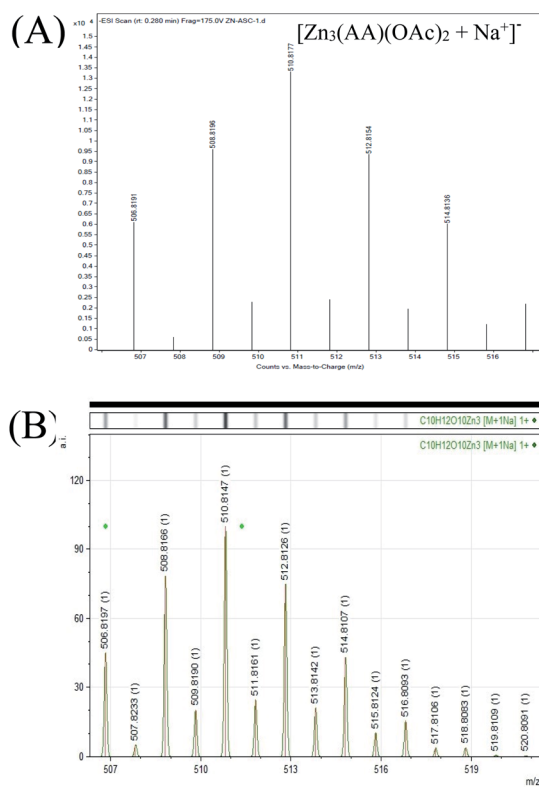


Fig. 8 (A) Experimental mass spectrum of the luminescent dispersion indicating the presence of  $\text{Zn}_3(\text{AA})(\text{OAc})_2$ . (B) Simulated mass spectrum of  $\text{Zn}_3(\text{AA})(\text{OAc})_2$ .

abundance ratio) of the luminescent samples were found to be in agreement with the simulated mass spectra of  $\text{Zn}_3(\text{AA})(\text{OAc})_2 + \text{Na}^+$  (Fig. 8A and B). Interestingly, the mass corresponding to the presence of  $\text{Zn}_3(\text{AA})(\text{OAc})_2$  was calculated to be 510.8147, which was in perfect agreement with the observed mass of 510.8177. Further, additional masses, consistent with the proposed structure of  $\text{Zn}_x(\text{AA})_y(\text{OAc})_z$  were also obtained (Fig. S9 and S10<sup>†</sup>). Also, the various observed and simulated masses of  $\text{Zn}_x(\text{AA})_y(\text{OAc})_z$  have been given in the ESI<sup>†</sup> in the tabulated form (Table S1<sup>†</sup>). The observed masses are consistent with the proposed structure. The results thus substantiated the critical roles of both  $\text{Zn}^{2+}$  and acetate ions (in addition to ascorbate) in the luminescence of the new species. It is to be noted here that analogous complexes of ascorbate ions with platinum are well established in the literature. Further, complexes of platinum with ascorbate ions are known to exist in multiple stoichiometric ratios. For instance, the reaction between platinum salt, alkyl diamine and ascorbic acid is known to give a mixture of products with a composition such as  $[\text{Pt}(\text{cis-amine})(\text{ascorbate})] \cdot 3\text{H}_2\text{O}$  as well as  $[\text{Pt}(\text{cis-amine})(\text{ascorbate})_2] \cdot 2\text{H}_2\text{O}$ .<sup>37</sup> Antitumor properties of such complexes have also been demonstrated.<sup>38</sup> Further, the detailed mechanism of the formation of platinum ascorbate complexes has also been established in the literature. Thus, the formation of a complex of  $\text{Zn}^{2+}$  ions with ascorbate and acetate is consistent with that in the literature.

Further, the NMR spectra of the mixture containing zinc acetate dihydrate and ascorbic acid in  $\text{D}_2\text{O}$  were acquired. The

observed chemical shifts of the protons of the resultant species were nearly concordant with the reported chemical shifts of the protons of zinc ascorbate (Fig. 9).<sup>39</sup> For example, the protons marked as ( $\text{H}_c$  and  $\text{H}_d$ ) and  $\text{H}_b$  appeared at  $\delta$  values of 3.56 and 3.84, respectively, whereas the literature reports of the  $\delta$  values of these protons (corresponding to zinc ascorbate) are at 3.65–3.70 and 3.97, respectively, with similar splitting patterns.<sup>39</sup> It may be noted here that the geminal protons in ascorbic acid ( $c$ ,  $d$ ) are known to undergo a second order splitting and hence appear as multiplets.<sup>40</sup> In addition, the chemical environment of the methylene protons might have been altered upon the complexation reaction between adjacent hydroxyl groups and zinc ions. This might have led to further geminal splitting (doublet of doublet) of the peak centred at 3.84 ppm. Further, the peak corresponding to 3.56 ppm appeared as a clear doublet of doublets as a consequence of vicinal coupling of two non-equivalent methylene protons. The results supported the reaction induced modification of the chemical environment

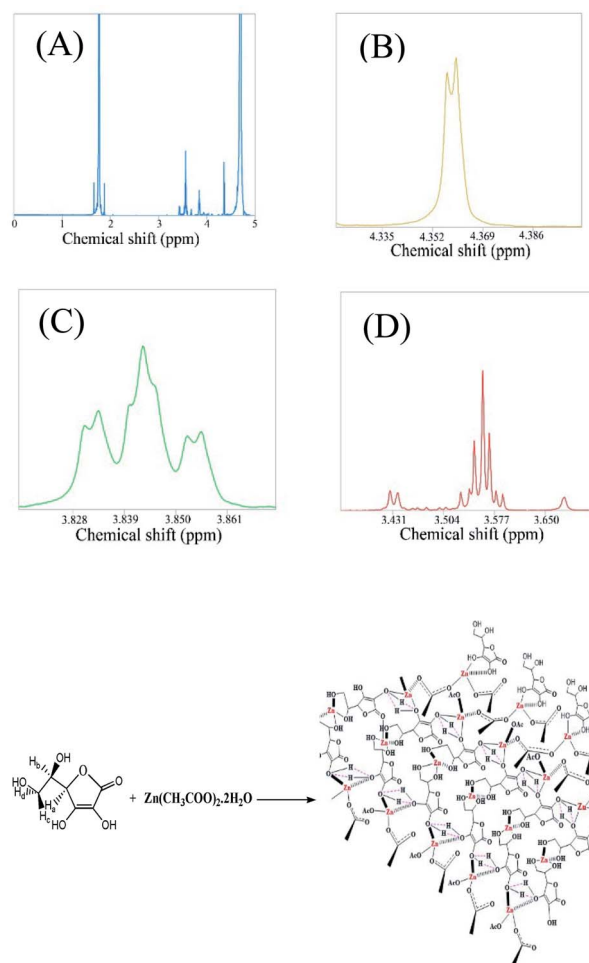


Fig. 9 (A) NMR spectrum of  $\text{Zn}_x(\text{AA})_y(\text{OAc})_z$ . (B) Magnified view of the peak shown in (A) at 4.35 for  $\text{H}_a$ . (C) Magnified view of the peak shown in (A) at 3.84 for  $\text{H}_b$ . (D) Magnified view of the peak shown in (A) at 3.56 for  $\text{H}_c$  and  $\text{H}_d$ . A schematic representation of the nanoparticle formation from the reaction between ascorbic acid and zinc acetate dihydrate.



around the above mentioned protons. This clearly indicated the variation in the chemical environment of protons of ascorbic acid and acetate, which is a typical signature of the complexation reaction.<sup>41</sup> Further, the protons of zinc ascorbate, marked herein as H3, were observed to appear at a  $\delta$  value of 4.35, which did match well with the reported value of 4.48 (Fig. 9D). The peak centred at 4.35 ppm appeared as a doublet due to first order geminal coupling. In addition, the peaks due to the protons of the acetate group were observed to be remarkably shifted *vis-à-vis* the peak due to protons of the zinc acetate peak (1.75); (Fig. S11†). This also confirmed the role of acetate as a constituent of the luminescent zinc ascorbate complex formed as a product of the reaction between zinc acetate and ascorbic acid. Chemical shifts of  $Zn_x(AA)_y(OAc)_z$  *vis-à-vis* ascorbic acid and zinc acetate dihydrate have been shown in Fig. S11A–D.† Thus the ESI-MS results in conjunction with the NMR results suggested the presence of  $Zn_x(AA)_y(OAc)_z$  as the building block of the luminescent nanoparticles observed in the TEM images. The chemical shifts of the protons of ascorbic acid and acetate upon the formation of  $Zn_x(AA)_y(OAc)_z$  have been given in the ESI† in the tabulated form (Table S2†).

The yield of the reaction was calculated from the area under the curve of the proton NMR peaks corresponding to the acetate ions at 0 h and 24 h of reaction. The calculated yield was found to be 14.87% (Fig. 10).

Moreover, Fourier transformed infrared (FTIR) spectroscopy analysis was performed to gain an insight into the plausible modes of bonding amongst zinc, acetate and ascorbate ions (Fig. S12†). Notably, the peaks due to the C=O and C=C ( $1757\text{ cm}^{-1}$  and  $1646\text{ cm}^{-1}$ ) stretching frequencies in ascorbic acid were found to be absent in the FTIR spectrum of  $Zn_x(AA)_y(OAc)_z$  NPs. This indicated the possible role of the aforementioned functional groups responsible for the association of ascorbate moieties resulting in the formation of nanoparticles. Importantly, the discrete peaks due to the OH groups ( $3212\text{ cm}^{-1}$ ,  $3309\text{ cm}^{-1}$ ,  $3400\text{ cm}^{-1}$  and  $3518\text{ cm}^{-1}$ ) in ascorbic acid were found to have been altered into a broad peak at  $3089\text{ cm}^{-1}$  in the FTIR spectrum of  $Zn_3(AA)(OAc)_2$  nanoparticles. This indicated the possible coordination between zinc ions and the OH groups of ascorbic acid, leading to the formation of nanoparticles. Further, the coordination among the hydroxyl oxygen of ascorbic acid and zinc ions was likely to affect the stretching frequencies of C–H bonds in the vicinity. Thus, a distinct disappearance of the peaks at  $3016\text{ cm}^{-1}$ , owing to the C–H bond vibrations of ascorbic acid, was observed following reaction with zinc ions. Importantly, the difference in wavenumbers for asymmetric and symmetric stretching frequencies of the acetate group in  $Zn_x(AA)_y(OAc)_z$  nanoparticles increased to  $132\text{ cm}^{-1}$  ( $\nu_a\ 1550\text{ cm}^{-1}$ ;  $\nu_s\ 1418\text{ cm}^{-1}$ ) from  $106\text{ cm}^{-1}$  ( $\nu_a\ 1543\text{ cm}^{-1}$ ;  $\nu_s\ 1437\text{ cm}^{-1}$ ) due to the precursor zinc acetate. This result clearly supports the switching of the bidentate chelating nature of the acetate group (in zinc acetate) to the bidentate bridging nature (in  $Zn_x(AA)_y(OAc)_z$  nanoparticles).

Interestingly, the so formed nanoparticulate zinc complex of ascorbate and acetate, was found to exhibit excitation tuneable emission. As shown in Fig. 11, upon gradually tuning the

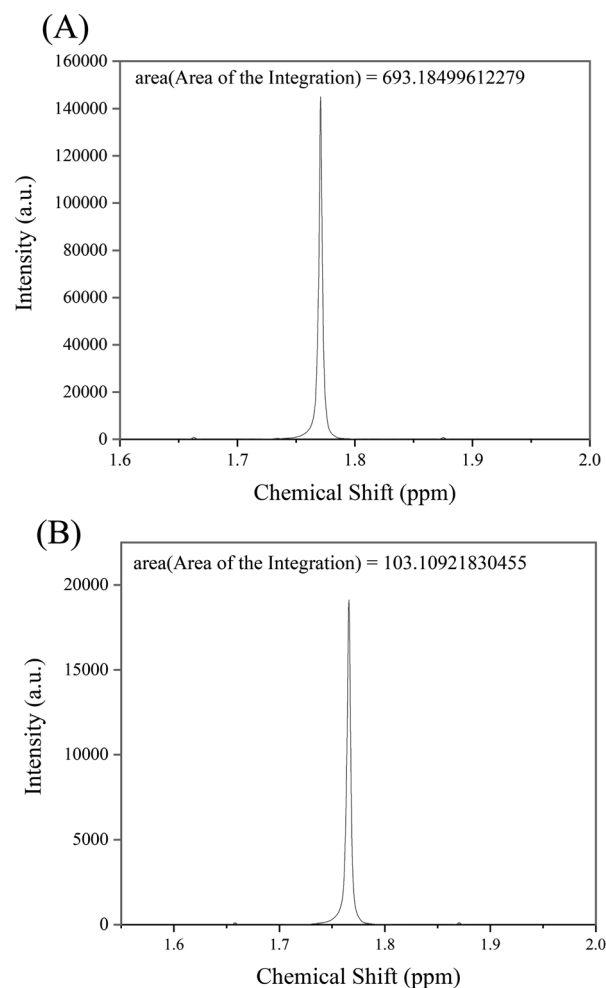


Fig. 10 Area of integration calculated for the NMR peaks of protons corresponding to acetate ions for the samples at (A) 0 h and (B) 24 h of reaction, respectively.

excitation wavelength from 365 to 400 nm, the emission maximum of the luminescent product (dispersion prepared following centrifugation and washing) shifted from 449 nm to 470 nm. Although understanding the origin of the excitation dependent emission properties of  $Zn_x(AA)_y(OAc)_z$  demands further investigation, the observed phenomenon may possibly be explained based on factors leading to excitation tuneable emission in the case of carbon dots.<sup>42</sup> As predominant in other forms of nanoscale particles, the possibility of existence of surface trap states in the present case can be taken into consideration. This is because of the involvement of –OH groups of ascorbic acid and acetic acid in the formation of  $Zn_x(AA)_y(OAc)_z$  nanoparticles. Also,  $sp^2$  and  $sp^3$  carbons of ascorbic acid may add to the possible existence of surface trap states.<sup>43</sup> These surface states, if exist at all, may lead to the availability of a wide range of energy levels. This might also lead to the emergence of excitation dependent luminescence of  $Zn_x(AA)_y(OAc)_z$  nanoparticles. Moreover, abundance of solvent (water) molecules around the nanoparticles may induce a number of emissive states to the system, which may also



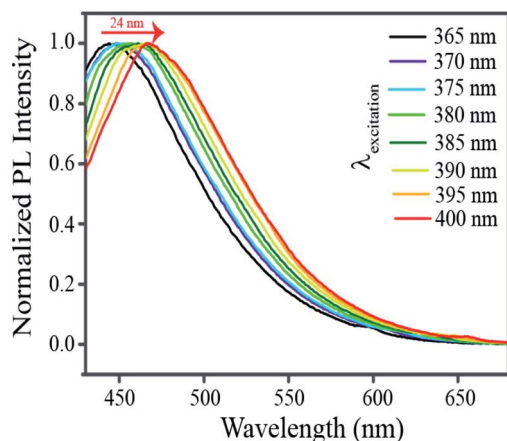


Fig. 11 Normalized emission spectra of the product of the reaction among  $\text{Zn}^{2+}$ , acetate ions and ascorbate ions with varying excitation (wavelengths) as mentioned in the legends.

contribute to the excitation tunable emission properties.<sup>44</sup> Now it may be argued here that the origin of luminescence in the nanoparticulate species could be due to the “aggregation induced emission” (AIE) of ascorbic acid. In order to probe this possibility, the emission spectra of the luminescent dispersion were acquired following serial dilutions. The results are reported in Fig. S13.† Thus, following sequential dilution, no significant change in the position of the emission maximum was observed. Only, the luminescence intensity of the dispersion was observed to have decreased following dilution of the luminescent dispersion (Fig. S13.†). In the case of molecules leading to AIE, generally, the peak due to AIE is reported to disappear upon dilution. However, in the current study, no such alteration in the luminescence spectra of the species could be observed. Thus, the emission characteristics observed herein were possibly due to the nanoscale particles of the complex formed from  $\text{Zn}^{2+}$ , acetate and ascorbate ions. Thus, the nanoscale particles of such a complex can lead to extraordinary emission and the excitation wavelength tuneability of that could also hold a clue to the emission characteristics of carbon dots.

The results presented above suggest that an aqueous mixture of ascorbic acid and zinc acetate underwent a chemical reaction leading to the formation of inorganic complexes with the formula  $\text{Zn}_x(\text{AA})_y(\text{OAc})_z$ . The reaction between ascorbic acid and zinc acetate led to the formation of nanoparticles of varying sizes having an absorption peak at 371 nm and exhibiting excitation tunable photoluminescence. The nanoparticles so formed were constituted of  $\text{Zn}_x(\text{AA})_y(\text{OAc})_z$  as the building unit. Also, as evinced from the FTIR analysis, hydrogen bonding might have played a prominent role in the association of the  $\text{Zn}_x(\text{AA})_y(\text{OAc})_z$  units, leading to the formation of complex nanoparticles. Although elucidating the exact origin of photoluminescence in the complex nanoparticles of  $\text{Zn}_x(\text{AA})_y(\text{OAc})_z$  is rather difficult and requires further investigation, as mentioned in the earlier section, a possible mechanism of luminescence may be attributed to the contribution of the surface states. It could be that, akin to carbon dots, the C=O functional groups

present in the acetate moieties might have introduced newer energy levels (HOMO) and facilitated the transition of electrons from the HOMO to the LUMO, the decay of which could be probed based on emission in the visible wavelengths. Another possibility could be that, in line with quantum dots, the crystalline boundary of the weak crystalline complexes of  $\text{Zn}_x(\text{AA})_y(\text{OAc})_z$ , at the nanoscale, might have significantly governed the electron distribution of the nanocomplexes – known as the quantum confinement effect – thereby leading to the electronic transition of the complex nanoparticles in the visible range. The presence of varied sizes in the medium might account for the wavelength tuneable emission. However, the exact mechanism of the photoluminescence is to be established through further work and evidence.

## Conclusion

In summary, we have developed a new luminescent nanoparticulate system comprising  $\text{Zn}_x(\text{AA})_y(\text{OAc})_z$  as the building unit. We have shown for the first time that nanocrystals of inorganic complexes may also exhibit quantum behavior akin to other systems like quantum dots, atomic clusters and carbon dots. The process of nanoparticle formation upon reaction of zinc acetate dihydrate and ascorbic acid has been demonstrated using transmission electron microscopy. It was found that the size of the nanoparticles evolved with time. The nanoparticle formation was preceded by the complexation reaction involving zinc, acetate and ascorbate ions. In addition, the control experiments indicated the importance of acetate ions in the formation of luminescent nanoparticles. The so formed nanoparticles, similar to carbon dots, exhibited excitation tuneable emission. The composition of the building block of the so formed nanoparticles was substantiated by ESI-MS and NMR analyses and was found to be  $\text{Zn}_x(\text{AA})_y(\text{OAc})_z$ . Experiments also suggested the critical role of the acetate ions in the complexation reaction, followed by crystallization leading to the emergence of new luminescent properties. The discovery of a new luminescent species based on nanoparticles of inorganic complexes provides an impetus to pursue further work in the field, which might provide interesting and important results. More importantly, the work portends to offer important leads with regard to the emergence of new properties at the nanoscale, for crystallization of molecules as bulk precipitate.

## Conflicts of interest

There are no conflicts to declare.

## Acknowledgements

We thank the Department of Electronics and Information Technology, Government of India [Grant 5(9)/2012-NANO, Vol. IV], for financial support. Arun Chattopadhyay thanks the Science and Engineering Research Board, Department of Science and Technology, for a J. C. Bose Fellowship (JCB/2019/000039). In addition, assistance from Central Instruments



Facility, IIT Guwahati, is acknowledged. We thank Dr Akshai Kumar A. S. for helpful discussions.

## Notes and references

- D. A. Hanifi, N. D. Bronstein, B. E. Koscher, Z. Nett, J. K. Swabeck, K. Takano, A. M. Schwartzberg, L. Maserati, K. Vandewal, Y. V. D. Burgt, A. Salleo and A. P. Alivisatos, *Science*, 2019, **363**, 1199–1202.
- S. Ye, A. P. Brown, A. C. Stammers, N. H. Thomson, J. Wen, L. Roach, R. J. Bushby, P. L. Coletta, K. Critchley, S. D. Connell, A. F. Markham, R. Brydson and S. D. Evans, *Adv. Sci.*, 2019, 1900911.
- Y. M. Su, Z. Wang, G. L. Zhuang, Q. Q. Zhao, X. P. Wang, C. H. Tung and D. Sun, *Chem. Sci.*, 2019, **10**, 564–568.
- R. Jin, C. Zeng, M. Zhou and Y. Chen, *Chem. Rev.*, 2016, **116**, 10346–10413.
- A. D. Kurdekar, L. A. A. Chundri, C. S. Manohar, M. K. Haleyrigirisetty, I. K. Hewlett and K. Venkataramaniah, *Sci. Adv.*, 2018, **4**, 6280.
- L. Xiao and H. Sun, *Nanoscale Horiz.*, 2018, **3**, 565–597.
- J. K. Lee, D. Samanta, H. G. Nam and R. N. Zare, *Nat. Commun.*, 2018, **9**, 1562.
- Y. He, J. C. Liu, L. Luo, Y. G. Wang, J. Zhu, Y. Du, J. Li, S. X. Lao and C. Wang, *Proc. Natl. Acad. Sci. U. S. A.*, 2018, **115**, 7700–7705.
- W. Zhou, X. Gao, D. Liu and X. Chen, *Chem. Rev.*, 2015, **115**, 10575–10636.
- J. Mosquera, M. Henriksen-Lacey, I. Gracia, M. Martinez-Calvo, J. Rodriguez, J. L. Mascarenas and L. M. Liz-Marzan, *J. Am. Chem. Soc.*, 2018, **140**, 4469–4472.
- J. H. Yoon, F. Selbach, L. Schumacher, J. Jose and S. Schüler, *ACS Photonics*, 2019, **6**, 642–648.
- M. K. Choi, J. Yang, T. Hyeon and D. H. Kim, *npj Flexible Electron.*, 2018, **2**, 10.
- Y. Jiang, S. Y. Cho and M. Shim, *J. Mater. Chem. C*, 2018, **6**, 2618–2634.
- Y. Lu, Y. Yin, B. T. Mayers and Y. Xia, *Nano Lett.*, 2002, **2**, 183–186.
- H. L. Chee, C. R. R. Gan, M. Ng, L. Low, D. G. Fernig, K. K. Bhakoo and D. Paramelle, *ACS Nano*, 2018, **12**, 6480–6491.
- K. L. Chen and M. Elimelech, *Langmuir*, 2006, **22**, 10994–11001.
- O. Zhou, H. Shimoda, B. Gao, S. Oh, L. Fleming and G. Yue, *Acc. Chem. Res.*, 2002, **35**, 1045–1053.
- P. T. Yin, S. Shah, M. Chhowalla and K. B. Lee, *Chem. Rev.*, 2015, **115**, 2483–2531.
- T. Liu and Z. Liu, *Adv. Healthcare Mater.*, 2018, **7**, 1701158.
- D. Lee, G. Monin, N. T. Duong, I. Z. Lopez, M. Bardet, V. Mareau, L. Gonon and G. D. Paëpe, *J. Am. Chem. Soc.*, 2014, **136**, 13781–13788.
- G. Almeida, I. Infante and L. Manna, *Science*, 2019, **364**, 833–834.
- D. Yang, M. Cao, Q. Zhong, P. Li, X. Zhang and Q. Zhang, *J. Mater. Chem. C*, 2019, **7**, 757–789.
- Y. Dong, Y. Zhao, S. Zhao, Y. Dai, L. Liu, Y. Li and Q. Chen, *J. Mater. Chem. A*, 2018, **6**, 21729–21746.
- W. Bae, S. Kocabay and T. Liedl, *Nanotoday*, 2019, **26**, 98–107.
- S. Huo, H. Li, A. J. Boersma and A. Herrmann, *Adv. Sci.*, 2019, **6**, 10.
- N. Xie, S. Liu, H. Fang, Y. Yang, K. Quan, J. Li, X. Yang, K. Wang and J. Huang, *ACS Nano*, 2019, **13**, 4174–4182.
- J. M. Sanfrutos, M. Ortega-Munoz, J. Lopez-Jaramillo, F. Hernandez-Mateo and F. Santoyo-Gonzalez, *J. Org. Chem.*, 2008, **73**, 7772–7774.
- J. Yang, A. Bahreman, G. Daudey, J. Bussmann, R. C. L. Olsthoorn and A. Keos, *ACS Cent. Sci.*, 2016, **2**, 621–630.
- A. K. Rengan, A. B. Bukhari, A. Pradhan, R. Malhotra, R. Banerjee, R. Srivastava and A. De, *Nano Lett.*, 2015, **15**, 842–848.
- G. A. Dichello, T. Fukuda, T. Maekwa, R. L. D. Whitby, S. V. Mikhalovsky, M. Alavijeh, A. S. Pannala and D. K. Sarker, *Eur. J. Pharm. Sci.*, 2017, **105**, 55–63.
- P. Sudhagar and T. P. Radhakrishnan, *J. Mater. Chem. C*, 2019, **7**, 7083–7089.
- S. Jayanty and T. P. Radhakrishnan, *Chem.–Eur. J.*, 2004, **10**, 2661–2667.
- L. Zong, H. Zhang, Y. Li, Y. Gong, D. Li, J. Wang, Z. Wang, Y. Xie, M. Han, Q. Peng, X. Li, J. Dong, J. Qian, Q. Li and Z. Li, *ACS Nano*, 2018, **12**, 9532–9540.
- X. Feng, Z. Xu, C. Qi, D. Luo, X. Zhao, Z. Mu, C. Redshaw, J. W. Y. Lam, D. Ma and B. Z. Tang, *J. Mater. Chem. C*, 2019, **7**, 2283–2290.
- Z. Q. Cao, Q. Miao, Q. Zhang, H. Li, D. H. Qu and H. Tian, *Chem. Commun.*, 2015, **51**, 4973–4976.
- G. G. Ramirez, D. A. Leigh and A. J. Stephens, *Angew. Chem., Int. Ed.*, 2015, **54**, 6110–6150.
- L. S. Hollis, A. R. Amundsen and E. W. Stern, *J. Am. Chem. Soc.*, 1985, **107**, 274–276.
- M. J. Arendse, G. K. Anderson and N. P. Rath, *Inorg. Chem.*, 1999, **38**, 5864–5869.
- C. Unaleroglu, B. Zumreoglu and K. Y. Mert, *J. Mol. Struct.*, 2002, **605**, 227–233.
- R. S. Reid, *J. Chem. Educ.*, 1989, **66**, 344.
- J. C. Ott, H. Wadepohl, M. Enders and L. H. Gade, *J. Am. Chem. Soc.*, 2018, **140**, 17413–17417.
- B. V. Dam, H. Nie, B. Ju, E. Marino, J. M. J. Paulusse, P. Schall, M. Li and K. Dohnalová, *Small*, 2017, **13**, 1702098.
- L. Li and T. Dong, *J. Mater. Chem. C*, 2018, **6**, 7944–7970.
- S. Khan, A. Gupta, N. C. Verma and C. K. Nandi, *Nano Lett.*, 2015, **15**, 8300–8305.

